Three-Dimensional Reconstruction of Nb_3Sn Films by Focused Ion Beam Cross Sectional Microscopy

E. Viklund, J. Lee, D. N. Seidman, and S. Posen

***Abstract*—Niobium has been the material of choice for SRF cavities for several decades due to its formability and superconducting properties. The accelerating gradient of niobium cavities is, however, rapidly approaching a theoretical limit. To achieve higher accelerating gradients a new material is needed that can sustain high fields. Nb_3Sn is a promising competitor with a higher superconducting transition temperature and a higher critical field than pure niobium. However, Nb_3Sn is very brittle and cannot be formed readily into a cavity. The main method for creating Nb_3Sn cavities is to form a Nb_3Sn film into a niobium surface using a tin vapor-diffusion method. This technique creates a microcrystalline Nb_3Sn thin film on the inner surface of the cavity. Tin depleted regions are known to form in the film during this process. Previous studies have analyzed these regions using transmission electron microscopy on cross-sectional lamellae prepared by focused ion beam/scanning electron microscope (FIB/SEM). This method does not provide any three-dimensional (3-D) information about the distribution of tin-deficient regions. In this study we employ a focused ion beam tomographic technique to analyze the 3-D structure of the film. Electron dispersive X-ray spectroscopy is used to image the tin concentration of the film in 3-D. Tin-deficient regions are discovered close to the surface of the Nb_3Sn film.**

***Index Terms*—Accelerator RF systems, niobium alloys, SRF cavity manufacturing, SRF superconducting radiofrequency cavities, thin films.**

I. Introduction

Nb_3Sn is a useful material for SRF cavities because it has a higher critical superconducting transition temperature (T_c) and superheating field (H_{sh}). Research on Nb_3Sn SRF cavities is motivated by their ability to achieve a high quality-factor, greater than 10^{10} at an operating temperature of 4 K, and high theoretical maximum accelerating gradient up to 100 MV/m. Despite the potential for higher accelerating gradients, Nb_3Sn cavities have been limited to the 10–20 MV/m range with the highest performing cavities achieving 24 MV/m [1]. The reason for this limited performance is thought to be due to imperfections formed during the manufacturing process of Nb_3Sn cavities.

Tin vapor-diffusion is the method of manufacturing Nb_3Sn SRF cavities that has produced the highest performing cavities to date. A thin film of Nb_3Sn is formed into the surface of niobium cavities through a tin-vapor reaction at elevated temperatures [1], [6]. Nb_3Sn grains nucleate and grow until the surface is completely covered. Once the surface is covered in an initial thin layer of Nb_3Sn, the film continues to grow via tin diffusion through Nb_3Sn grain boundaries (GBs) [6].

The result is an imperfect film of Nb_3Sn. Analysis of the film shows that it contains areas with low tin concentration known as tin-depleted regions [2]. Depending on the coating parameters, the GBs may also be tin-rich or tin-deficient [3]. These stoichiometric differences can depress the critical superconducting transition temperature (T_c) of the material from 18 K down to as low as 6 K depending on the concentration of anti-site defects [4]. A lower T_c causes an increase in the surface resistance of the cavity and makes it more likely to quench.

In addition to stoichiometric imperfections, the tin-vapor diffusion coated Nb_3Sn films also have micro-scale surface roughness caused by faceting of the grains and thermal etching at the grain boundaries. Surface roughness concentrates the magnetic field around sharp edges on the surface, thereby exceeding the critical field of the Nb_3Sn prematurely [5]. The interface between the film and the niobium substrate is also uneven because of the interfacial reaction between niobium and tin [2]. The film can become too thin in some areas, allowing the RF fields to interact with the niobium substrate and poorly superconducting Nb-Sn phases at the interface.

The 3-D structure of the Nb_3Sn film becomes especially important when material is removed from the surface by polishing. Efforts have been made to polish Nb_3Sn using electropolishing [13], buffered chemical polishing [13], and oxypolishing [14]. These techniques remove material from the surface of the film, which could expose subsurface tin-deficient regions. Polishing is an important step for improving the performance of niobium SRF cavities and will likely become an important step for Nb_3Sn SRF cavity manufacturing in the future.

The structure of vapor diffusion coated Nb_3Sn films has been studied by many people using transmission and scanning electron-microscopy (TEM and SEM) [2], [7], [8], [9], and X-ray photo-emission spectroscopy (XPS). [6], [10], [11]. These techniques provide 2-D or 1-D information about the chemical composition in the film and are therefore unable to determine

Manuscript received 12 November 2022; revised 6 March 2023; accepted 10 March 2023. Date of publication 16 March 2023; date of current version 28 March 2023. This work was supported by Fermi Research Alliance, LLC under Grant DE-AC02-0 6857737CH11359 with the U.S. Department of Energy, Office of Science, Office of High Energy Physics. *(Corresponding author: E. Viklund.)*

E. Viklund and D. N. Seidman are with the Northwestern University Department of Materials Science and Engineering, Evanston, IL 60208 USA (e-mail: ericviklund2023@u.northwestern.edu).

J. Lee and S. Posen are with the Fermi National Accelerator Laboratory, Batavia, IL 60510 USA.

Color versions of one or more figures in this article are available at https://doi.org/10.1109/TASC.2023.3257819.

Digital Object Identifier 10.1109/TASC.2023.3257819

the 3-D distribution of tin-deficient regions. We cannot reliably determine how many of these regions are interacting with the RF fields, and we cannot determine their effects on cavity performance using the currently available data.

In this study, we used a 3-D imaging method, focused ion-beam (FIB) tomography, to measure the distribution of tin inside vapor-diffusion coated Nb_3Sn films to search for Sn-deficient regions and determine their impact on the performance of Nb_3Sn vapor-diffusion coated cavities.

II. Method

FIB tomography is a measurement technique that utilizes a combined FIB/SEM instrument. This facilitates rapid switching between e-beam imaging and ion-beam milling. The ion-beam is tilted 52° relative to the e-beam. During sample preparation and imaging, the stage is tilted 52° so that the ion-beam is perpendicular to the sample's surface. A protective, 2 μm thick Pt capping layer is deposited over the region-of-interest (ROI) to prevent damage from the ion-beam over the course of the measurement. The sample is prepared by ion-beam milling a trench to expose a cross-section of the sample surface. Then a clearance trench is milled on both sides of the ROI to ensure direct line-of-sight between the cross-section and the detector. This prevents shadows from forming in the e-beam image. Once the sample is prepared, the e-beam is employed to image the cross-section. An automated process alternates between using the ion-beam to mill a thin layer of material, creating a new cross-section, and imaging each cross-section using the e-beam. The individual e-beam images are then combined to create a 3-D image of the sample.

We employ energy dispersive X-ray spectroscopy (EDS) to measure the chemical composition of the sample. This method measures the emitted X-ray spectrum created by the e-beam when it is focused on a sample. Each element has a characteristic X-ray spectrum, which can be used to identify the chemical composition of the sample. To measure the distribution of tin in a sample, X-rays from the Sn Lα X-ray series are counted. Regions of high tin concentration will emit more of these characteristic X-rays compared to low tin concentration regions.

We utilized a ThermoFischer Helios 5 FIB/SEM microscope to obtain the measurement. A 30 kV, 2.7 nA Ga+ ion-beam is employed to mill the sample. The electron-beam current and accelerating voltage are 11 nA and 20 kV. X-rays from the Sn Lα series was counted by an Oxford Ultim EDS detector. With these beam parameters, the EDS detector was close to its maximum count rate of one million counts per second. The measured volume is approximately $20 \times 20 \times 7$ μm. The data was cropped to $17 \times 8 \times 6$ μm to remove artifacts at the boundaries. 20 nm slices were cut for each e-beam image and the pixel size was 20×25.4 nm. The 3-D data set was binned and smoothed with a Gaussian filter to minimize noise, yielding a final voxel size of $80 \times 80 \times 101.5$ nm.

The sample is a 1 cm diameter and 4 mm thick niobium disk coated with a 2 μm thick Nb_3Sn film produced by the vapor-diffusion process [6]. The samples were coated at 1100 °C in a tin-coating furnace at Fermi National Accelerator Laboratory (FNAL).

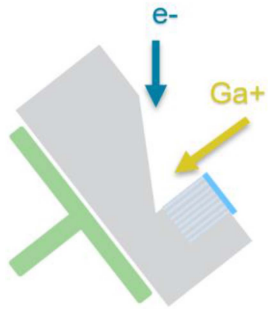

Fig. 1. A schematic showing the orientation of the electron-beam, ion-beam, and sample during a FIB tomography measurement. The blue region on the sample indicates the capping layer, and the light-blue lines in the sample indicate the slices milled by the ion-beam.

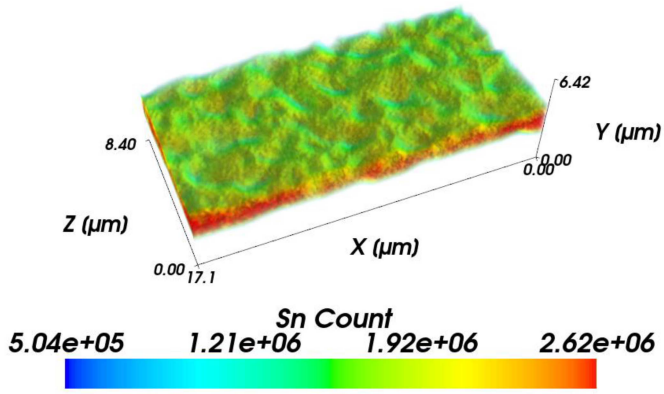

Fig. 2. The 3-D distribution of tin inside a vapor-diffusion coated Nb_3Sn film as determined from the Sn X-ray count originating from each point. The top surface visible in the figure is the Nb_3Sn-vacuum interface.

III. Results

Using the FIB tomography method, we were able to measure the 3-D distribution of tin inside a vapor-diffusion coated Nb_3Sn film. This distribution is presented in Fig. 2, rendered using a volumetric shading technique. The surface of the film is visible, but it is difficult to observe the internal structure of the film.

To better visualize the data, an iso-concentration surface is calculated. This surface intersects all the points in 3-D space with the same Sn X-ray signal intensity. From Fig. 3 the surface roughness of the film can be observed, and the roughness of the Nb_3Sn-Nb interface is also apparent.

The iso-surface is used to calculate the thickness of the film in the X-Z plane by projecting a ray perpendicular to the plane and determining the distance between the intersection points on the top and bottom surfaces of the Nb_3Sn. From the thickness calculation, we calculate statistical parameters of the film such as the mean, minimum, and maximum thickness. The mean film thickness of the Nb_3Sn film is 1.96 μm, but some areas are as thin as 0.72 μm.

To visualize the internal structure of the film, it is easier to analyze individual cross-sections of the data. Fig. 5 displays

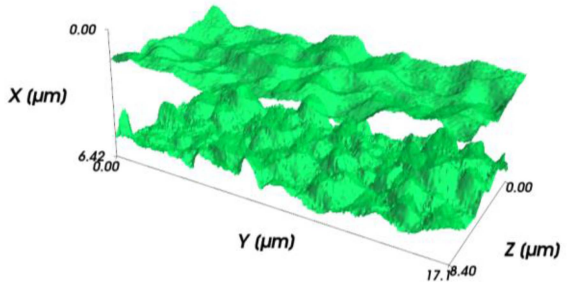

Fig. 3. The boundaries of the Nb3Sn film calculated from the 3-D Sn X-ray count distribution. The top surface is the Nb_3Sn-vacuum interface, and the bottom surface is the Nb_3Sn-Nb interface. The threshold value for the isoconcentration-surface was chosen as 1.5×10^6 counts.

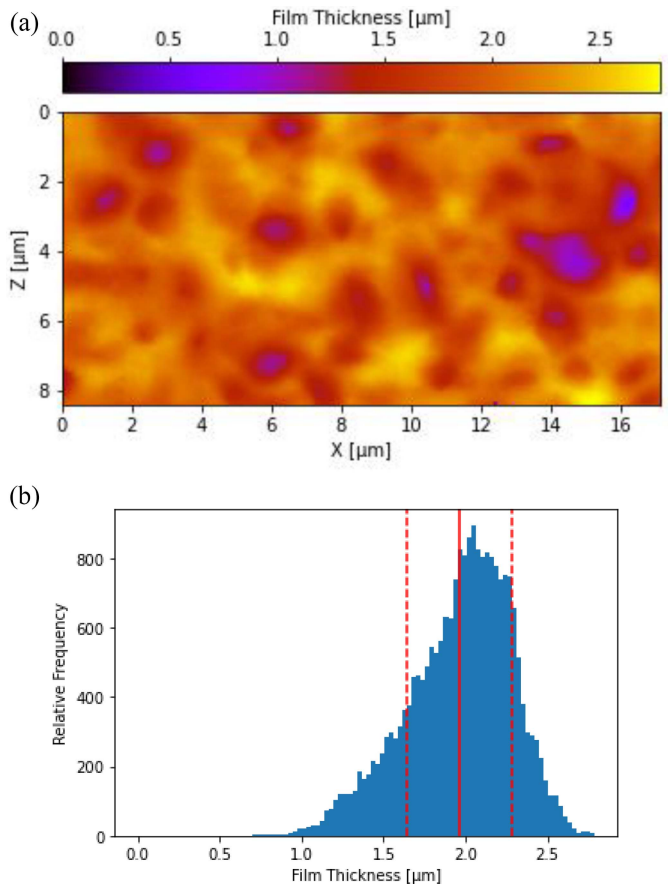

Fig. 4. (a) This figure shows the thickness of the Nb_3Sn film calculated from the Sn iso-surface. The X and Z axes are oriented in the in the plane of the Nb_3Sn film. (b) The histogram shows relative frequency of thicknesses across the measured surface of the Nb_3Sn film. The mean and standard deviation are indicated by a solid line and two dashed lines. The minimum thickness is 0.72 μm and the maximum thickness is 2.79 μm.

cross-sections of the 3-D image at different locations in the film. These cross-sections show several areas with low tin concentration including some areas that are within 200 nm of the film surface. There is also a region that shows a protrusion of the Nb substrate into the film and where the thickness of the film decreases to less than 1 μm. This is likely caused by a tin diffusion barrier in this region such as an unfavorable grain orientation or defects in the substrate.

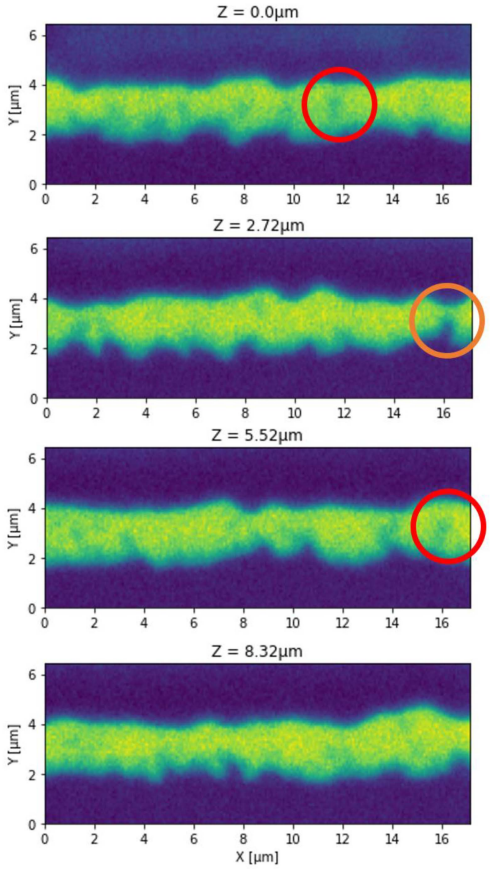

Fig. 5. Four different cross-sections of the 3-D EDS dataset are displayed. The axes are oriented as shown in Fig. 2. The Y-axis is perpendicular to the film and the X and Z axes lie in the plane of the film. The color of each pixel indicates the relative intensity of the Sn X-ray signal from the sample. A high signal corresponds to a yellow color, and a low signal corresponds to a dark-blue color. A thin region of the film is indicated by an orange-colored circle and two Sn-deficient regions are indicated by a red circle.

IV. Discussion

Our results demonstrate that Sn-deficient regions and thin regions occur frequently near the surface of vapor-diffusion coated Nb_3Sn films. We detected multiple regions where the Sn-concentration is less than the bulk Nb_3Sn concentration, and we also found that the film is as thin as 0.72 μm in some regions. This suggests that one cause of Nb_3Sn SRF cavity performance degradation could be the interaction of the RF field with poorly superconducting, off-stoichiometric phases. The effect of these defects on SRF cavity performance is expected to be negligible so long as they are far from the surface, outside the 89 nm penetration depth of Nb3Sn [15] or a few multiples thereof. Nb and Sn-deficient defects may also lower the T_c and superconducting energy gap of the film through the proximity effect, which occurs on the scale of the coherence length of Nb_3Sn, 5.7 nm [15], far smaller than the RF penetration depth. It is difficult to estimate the effect of these defects compared to other sources of degradation such as surface roughness.

The effects of these near-surface imperfections are expected to be more significant when applying a polishing treatment such as electropolishing, buffered chemical polishing, or mechanical

polishing, since these processes remove the top layer of stoichiometric Nb_3Sn and expose the imperfections, allowing them to interact more strongly with the RF field.

We also find that the film has large fluctuations thickness. Therefore, polishing using chemical methods would quickly expose the underlying niobium substrate, since the Nb_3Sn is as thin as 0.72 μm in some areas. Exposing the niobium substrate would increase the surface resistance of the cavity and potentially expose poorly superconducting Nb-Sn phases that exist near the interface [2].

To remove the tin-deficient regions, changes may need to be made to the vapor-diffusion coating parameters such as adjusting the temperature, coating duration, or changing the amount of tin vapor in the furnace to allow for tin diffusion into these off-stoichiometry regions. For polished Nb_3Sn films, the cavities could be reintroduced into the coating furnace to apply a new layer of tin to the surface which can react with the exposed tin-deficient regions and form a new layer of stoichiometric Nb_3Sn on the surface.

The FIB Tomography method described in this paper also needs improvement. We would like to calculate statistical parameters about the size and distribution of the tin-depleted regions, but the contrast between the tin-deficient regions and the bulk Nb_3Sn is too low to programmatically distinguish the regions consistently. The low contrast of the image can be attributed to a low signal-to-noise ratio of the Sn X-ray signal and low spatial resolution.

The low spatial resolution is caused by the large interaction volume of the electron-beam when using a high beam voltage, 20 kV, and high beam current, 11 nA. The X-rays are emitted from the entire interaction volume leading to blurring of the boundaries between areas of different chemical composition. Reducing the beam current and acceleration voltage will improve the spatial resolution and the sensitivity of the measurement to small changes in tin concentration.

The signal-to-noise ratio of the measurement can also be improved by using the Nb Lα X-ray signal to measure the local Nb-Sn ratio. The Nb Lα X-rays have an energy of 2.2 keV compared to 3.4 keV for Sn Lα X-rays [12]. This difference in energy leads to a 10 times greater X-ray intensity from niobium compared to tin. By incorporating both types of X-rays, the total X-ray count will be increased leading to a higher signal-to-noise ratio and lower acquisition times.

V. Conclusion

Using FIB tomography we found that Sn-deficient regions and thin regions are a common feature of vapor-diffusion coated Nb_3Sn film. Additionally, we discovered that several of these regions are close to the surface of the film where they could interact with the RF field of the SRF cavity, especially if the film is chemically or mechanically polished. This suggests that sub-surface tin-deficient regions may play a role in degrading the performance of vapor-diffusion coated Nb_3Sn SRF cavities. Further research is required to quantify the effects of these sub-surface imperfections on the performance of Nb_3Sn SRF cavities. Methods of mitigating these regions, such as recoating the surface after polishing may need to be developed to achieve better performing SRF cavities. The FIB tomography methodology also needs to be optimized for imaging Nb_3Sn films and tin-deficient regions by improving the spatial resolution and signal-to-noise ratio of the measurement.

References

[1] S. Posen et al., "Advances in Nb_3Sn superconducting radiofrequency cavities towards first practical accelerator applications," *Supercond. Sci. Technol.*, vol. 34, no. 2, 2021, Art. no. 025007.

[2] J. Lee et al., "Atomic-scale analyses of Nb_3Sn on Nb prepared by vapor diffusion for superconducting radiofrequency cavity applications: A correlative study," *Supercond. Sci. Technol.*, vol. 32, no. 2, 2018, Art. no. 024001.

[3] J. Lee et al., "Grain-boundary structure and segregation in Nb_3Sn coatings on Nb for high-performance superconducting radiofrequency cavity applications," *Acta Materialia*, vol. 188, pp. 155–165, 2020.

[4] N. S. Sitaraman et al., "Effect of the density of states at the Fermi level on defect free energies and superconductivity: A case study of Nb_3Sn," *Phys. Rev. B*, vol. 103, no. 11, 2021, Art. no. 115106.

[5] R. Porter, D. L. Hall, M. Liepe, and J. T. Maniscalco, "Surface roughness effect on the performance of Nb_3Sn cavities," in *Proc. LINAC*, 2016, pp. 129–132.

[6] U. Pudasaini, G. V. Eremeev, J. W. Angle, J. Tuggle, C. E. Reece, and M. J. Kelley, "Growth of Nb_3Sn coating in tin vapor-diffusion process," *J. Vac. Sci. Technol. A: Vac., Surfaces, Films*, vol. 37, no. 5, 2019, Art. no. 051509.

[7] C. Becker et al., "Analysis of Nb_3Sn surface layers for superconducting radio frequency cavity applications," *Appl. Phys. Lett.*, vol. 106, no. 8, 2015, Art. no. 082602.

[8] D. L. Hall et al., "Surface analysis of features seen on Nb_3Sn sample coupons grown by vapour diffusion," in *Proc. IPAC*, 2017, pp. 1130–1133.

[9] D. L. Hall, J. J. Kaufman, M. Liepe, and J. Maniscalco, "Surface analysis studies of Nb_3Sn thin films," in *Proc. IPAC*, 2016, pp. 2316–2319.

[10] Z. Sun et al., "Fast Sn-ion transport on Nb surface for generating Nb_xSn thin films and XPS depth profiling," in *Proc. North Amer. Part. Accel. Conf.*, 2019, pp. 727–730.

[11] U. Pudasaini, G. Eremeev, C. E. Reece, J. Tuggle, and M. J. Kelley, "Effect of deposition temperature and duration on Nb_3Sn diffusion coating," in *Proc. 9th Int. Part. Accel. Conf.*, 2018, pp. 3950–3953.

[12] W. H. McMaster, N. K. Del Grande, J. H. Mallett, and J. H. Hubbell, "Compilation of X-ray cross sections," Jan. 1969. [Online]. Available: https://www.osti.gov/biblio/4794153

[13] H. Hu, "Reducing surface roughness of Nb_3Sn through chemical polishing treatments," in *Proc. Conf. RF Supercond.*, 2019, pp. 48–50.

[14] U. Pudasaini, G. Eremeev, C. E. Reece, J. Tuggle, and M. J. Kelley, "Studies of electropolishing and oxypolishing treated diffusion coated Nb_3Sn surfaces," in *Proc. 9th Int. Part. Accel. Conf.*, 2018, pp. 3954–3957.

[15] S. Keckert et al., "Critical fields of Nb_3Sn prepared for superconducting cavities," *Supercond. Sci. Technol.*, vol. 32, no. 7, 2019, Art. no. 075004.